# Study of Poly(amidoamine) Starburst Dendrimers by Fluorescence Probing

**ARTICLE** *in* LANGMUIR · OCTOBER 1997

Impact Factor: 4.46 · DOI: 10.1021/la970529i

# Study of Poly(amidoamine) Starburst Dendrimers by Fluorescence Probing

G. Pistolis, Angelos Malliaris,* C. M. Paleos, and D. Tsiourvas

*NRC "Demokritos", 15310 Athens, Greece*

*Received May 22, 1997. In Final Form: August 11, 1997*[⊗]

The binding of fluorescent probe molecules to poly(amidoamine) starburst dendrimers of generations G-0, G-1, and G-2 was investigated. The solubilizing capability of these new materials, in aqueous media, increases with increasing degree of their generation. Pyrene fluorescence however undergoes significant quenching in the solubilized state. In the higher generations, G-1 and G-2, excimer fluorescence was observed even at [pyrene]/[dendrimer] ratios as low as $10^{-3}$.

## I. Introduction

During the last few years there has been a growing interest for the development of macromolecules with morphological architectures differing from the typical linear polymers and the classical micelles which are formed by intermolecular aggregation. Dendritic macromolecules are hyperbranched polymers consisting of a central core and of a number of monomeric repeat units bearing a functional group, e.g., $NH_2$, which acts as a branching point for the development of the dendrimer (see Chart 1). Depending on the number of times the repeat unit is repeated in a dendrimer, structures of various so-called generations, viz., 0, 1, 2, 3, ..., are obtained, as depicted in Chart 1. These materials belong to a novel class of macromolecules synthesized in a simple stepwise procedure by a repetitive reaction sequence.[1] Numerous advantages characterize the above materials. First, dendrimers which are formed by covalent bonds have greater structural stability than conventional micelles. Second, depending on the synthetic strategy, a high degree of control over molecular weight and shape is achieved, leading to precise compositions and constitutions of these unimolecular entities. Third, since the exterior layer of a dendrimer contains chemically active groups (e.g., $NH_2$ in Chart 1), it may be modified covalently to provide a variety of functionalities leading to desired systems.

Several excellent reviews[1−10] have been published covering the topic from details to highlights and perspectives. Following the work on the synthesis of diversified dendrimers, investigations have recently started on the study of inclusion phenomena based on the concept of "dentritic boxes"[11,12] formed in the presence of guest molecules. On the other hand Fréchet and his co-workers have studied the dynamic solubilization of pyrene[8,13] in a water soluble dendrimer, and Tomalia et al. have shown with NMR relaxation studies that organic molecules, like

**Chart 1**

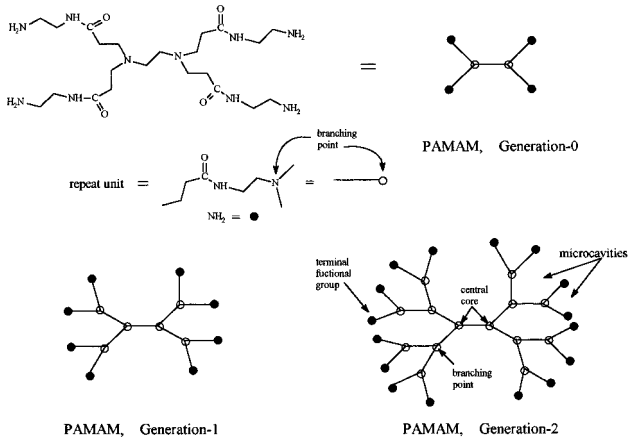


aspirin, can be introduced to the interior of the poly(amidoamines) starburst dendrimers (PAMAMs, generations 0−10).[14] Concerning the growing interest for developing efficient materials as controlled release systems of drugs in pharmaceutical and agrochemical science,[3] dendrimers look promising. Starburst poly(amidoamines) PAMAMs dendrimers (Chart 1) were originally prepared and characterized by Tomalia[1] and are among the first compounds to be commercially available.

Although starburst dendrimers possess a precise composition and constitution, there are no direct methods, e.g., X-ray crystallography, providing detailed data on their structure. However, molecular simulations[14] give some information concerning the key role of the degree of generation on molecular shape, morphology, and surface structure. Specifically, according to these molecular simulations "low" generations (0−2) possess a highly asymmetric, open, "starfish-like" shape, while the "high" generations ≥4 have a nearly spherical shape and present more closed and densely packed structures. The generation-3 possesses an intermediate structure which is neither asymmetric nor spherical. In view of the fact that the low generations have received little attention,[15] we have focused our studies on them in order to elucidate subtle molecular differentiations among the high asymmetric dendrimers of generations 0, 1, and 2. For this purpose

[⊗] Abstract published in *Advance ACS Abstracts,* October 1, 1997.

(1) Tomalia, D. A.; Naylor, A. M.; Goddard, W. A. *Angew. Chem., Int. Ed. Engl.* **1990**, *29*, 138.
(2) Dvornic, P. R.; Tomalia, D. A. *Macrom. Symp.* **1994**, *88*, 123.
(3) Ardoin, N.; Astruc, D. *Bull. Soc. Chim. Fr.* **1995**, *132*, 875.
(4) Mekelburger, H. B.; Jaworek, W.; Vogtle, F. *Angew. Chem., Int. Ed. Engl.* **1992**, *31*, 1571.
(5) Issberner, J.; Moors, R.; Vogtle, F. *Angew. Chem., Int. Ed. Engl.* **1994**, *33*, 2413.
(6) Voit, B. I. *Acta Polym.* **1995**, *46*, 87.
(7) Tomalia, D. A. *Adv. Mater.* **1994**, *6*, 529.
(8) Fréchet, J. M. J. *Science* **1994**, *263*, 1710.
(9) Zimmerman, S. C.; Zeng, F.; Reichert, D. E. C.; Kolotuchin, S. V. *Science* **1995**, *271*, 1095.
(10) Bell, T. W. *Science* **1995**, *271*, 1077.
(11) Jansen, J. F. G. A.; E. M. M. de Brabander-van den Berg; Meijer, E. W. *Science* **1994**, *266*, 1226.
(12) Jansen, J. F. G. A.; Meijer, E. W. *J. Am. Chem. Soc.* **1995**, *117*, 4417.
(13) Hawker, C. J.; Woolly, K. L.; Fréchet, J. M. J. *J. Chem. Soc., Perkin Trans.* 1 **1993**, 1287.
(14) Naylor, A. M.; Goddard, W. A.; Kiefer, G. E.; Tomalia, D. A. *J. Am. Chem. Soc.* **1989**, *111*, 2339.
(15) Caminati, G.; Turro, N. J.; Tomalia, D. A. *J. Am. Chem. Soc.* **1990**, *112*, 8515.

S0743-7463(97)00529-5 CCC: $14.00 

we have used pyrene fluorescence to explore (i) the ability of these dendrimers to interact with guest organic molecules, (ii) their binding capabilities, and (iii) the nature of their interior (dendritic box).

## II. Experimental Section

PAMAM dendrimers, generation 0, 1, and 2, were purchased from Aldrich and used without further purification, they were however examined by one- and two-dimensional NMR techniques. Pyrene was also purchased from Aldrich and was purified by zone melting. The two derivatives of DPH (1,6-diphenyl-1,3,5-hexatriene), viz., DPH−$NO_2$ and DPH−$N(CH_3)_2$, were obtained from Lambda Probes & Diagnostics and used as received. For absorption spectra the Perkin-Elmer Lamba-16 spectrophotometer was used, while fluorescence spectra were recorded on a Perkin-Elmer LS-50B fluorometer and lifetimes were determined with the FL900 single photon counter of Edinburgh Instruments. For pyrene the excitation wavelength was set at 335 nm where its extinction coefficient $\epsilon$ was found to be the same when pyrene is either free or complexed with the dendrimers. The maximum concentration of pyrene in water was found equal to $8.0 \times 10^{-7}$ M, in excellent agreement with previous studies.[16] Light scattering experiments were performed in a KMX-6 Laser instrument. It should be mentioned that aqueous solutions of all three dendrimers produce a weak fluorescence around 430 nm. To eliminate this impurity emission we always subtract from the fluorescence of pyrene the fluorescence of appropriate blanks containing the same dendrimer concentration as the samples. All the solutions of the organic fluorescence probes, either in pure water or in dendrimer aqueous solutions, were prepared by allowing the solvent to stay overnight undisturbed in contact with the solute, which had been previously deposited as a thin film on the bottom of an Erlenmeyer flask.

## III. Results and Discussion

**Solubilization and Micropolarity Studies.** It is well established that the aqueous solubility of hydrophobic molecules can be dramatically enhanced in the presence of water soluble surface active agents. Therefore dendrimers, which resemble unimolecular micelles, are expected to increase the solubility of water insoluble or weakly soluble organic compounds. Depending on the available number of microcavities, and the chemical composition of the repeat unit, the binding strength and the adsorption capacity of dendrimers may be altered according to their degree of generation. In the present study we have examined, by UV−VIS absorption spectroscopy, aqueous dendrimer solutions of generation 0, 1, and 2, saturated with pyrene. Under these conditions the concentration of the maximum solubilized pyrene was found to increase linearly with the size of the corresponding dendrimer, expressed either in terms of dendrimer molecular weight or in terms of the number of microcavities in each dendrimer. Thus, $10^{-2}$ M aqueous solutions of generation G-0 (MW = 516, no. of cavities = 2); G-1 (MW = 1429, no. of cavities = 6), and G-2 (MW = 3250, no. of cavities = 14) dendrimers, solubilize $1.1 \times 10^{-6}$, $2.64 \times 10^{-6}$, and $7.55 \times 10^{-6}$ M pyrene, respectively. We conclude therefore that the generation plays an important role in the association between pyrene and the dendrimer. Thus the amount of solubilized pyrene, and presumably of other organic molecules, can be controlled to some desired value by using dendrimers of the appropriate generation.

(16) Schwarz, *J. Chem. Eng. Data* **1977**, *22*, 399.

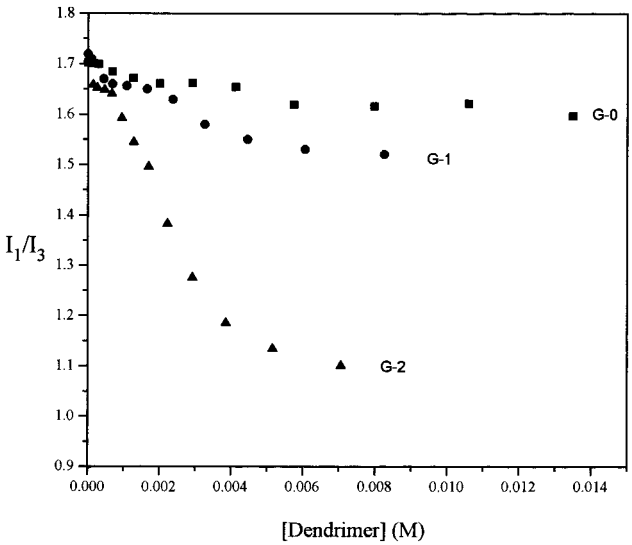


**Figure 1.** Variation of the intensity ratio of the first ($I_1$) to the third ($I_3$) pyrene fluorescence peaks vs the total added dendrimer concentration: ■, G-0; ●, G-1; ▲, G-2. Pyrene concentration = $8 \times 10^{-7}$ M.

In order to investigate the micropolarities at the solubilization sites of these dendrimers, we have used the $I_1/I_3$ ratio of the fluorescence intensity of the first to the third vibrational peak of pyrene, which is a well-known polarity index.[17] Figure 1 shows the variation of $I_1/I_3$ as a function of added dendrimer to an aqueous solution saturated with pyrene. It is clear that the dependence of the ratio on the dendrimer concentration changes significantly from G-0 to G-2. Thus, in the case of generation-0 there is but a small decrease in the value of $I_1/I_3$, in the case of G-1 this change is more evident, and in the case of G-2 the value of the ratio changes dramatically with increasing added dendrimer concentration.

The experimental results of Figure 1 are rationalized in terms of the extent of water penetration into the dendrimer microcavities. Thus, the G-0 dendrimer has only four repeat units and consequently possesses the smallest radius and a very open structure, which appears unable to protect pyrene molecules efficiently from the bulk aqueous phase. Generations 1 and 2, on the other hand have additional repeat units, and therefore larger structures, providing better water protection to the solubilized pyrene molecules. Note that the values of $I_1/I_3$ in G-0 and G-1 are close to those observed in pure water (ca. 1.50−1.60), whereas in G-2 $I_1/I_3$ has a value close to that in aqueous micelles (ca. 1.0−1.4).[18] The above observations were further confirmed using as probes two derivatives of the well-known fluorescent probe DPH, viz., DPH−$N(CH_3)$ and DPH−$NO_2$. These water insoluble probes exhibit strong fluorescence red shifts with increasing medium polarity, while the later is absolutely nonfluorescent in aqueous media.[18] In conclusion, pyrene, via the $I_1/I_3$ ratio, as well as DPH−$N(CH_3)_2$, via its red shift, shows that the local polarity in the microcavities of G-0 and G-1 is close to that of water, while in G-2 it is approximately equal to the polarity of ether.[19] Further evidence that in G-2 water hardly penetrates in the microcavities is provided by the fact that DPH−$NO_2$, which does not fluoresce in water,[18] emits from G-2 dendrimers but not from G-0 and G-1.

(17) Glushko, V.; Thaler, M. S. R.; Karp, C. D. *Arch. Biochem. Biophys.* **1981**, *33*, 210.
(18) Pistolis, G.; Malliaris, A. *Langmuir* **1997**, *13*, 1457.
(19) Kalyanasundaram, K.; Thomas, K. J. *J. Am. Chem. Soc.* **1977**, *99*, 2039.

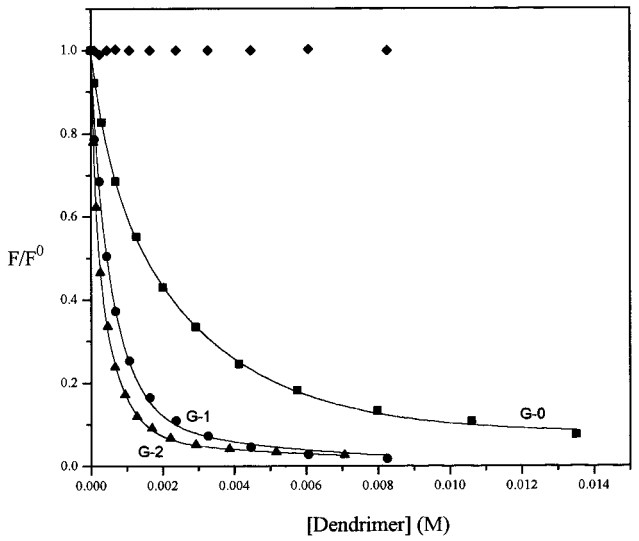


**Figure 2.** Plot of $F/F°$ vs the total added dendrimer concentration. $F°$ is the total fluorescence intensity of an aqueous pyrene solution ($8 \times 10^{-7}$ M), whereas $F$ stands for the intensity after each addition of the dendrimer. ■, G-0; ●, G-1; ▲, G-2; ◆, G-2 in an ethanolic pyrene solution ($8 \times 10^{-7}$ M). The lines through the experimental points are the best fitts obtained according to eq 8 (see text).

**Monomer Pyrene Fluorescence Quenching.** When any one of the dendrimers G-0, G-1, or G-2 was added to a dilute ($8 \times 10^{-7}$ M) aqueous solution of pyrene, a drastic decrease of the fluorescence intensity was observed, as shown in Figure 2. This loss of fluorescence intensity is not caused by some impurity existing in the dendrimer solutions as proved by the fact that when ethanol, instead of water, was employed as the solvent, the fluorescence intensity remained constant and independent of the amount of added dendrimer (see Figure 2). On the other hand, when either biacetylethylenediamine ($CH_3CONHCH_2CH_2NHCOCH_3$), which resembles the basic repeat unit of these PAMAM dendrimers, or ethylenediamine, which bears the terminal $NH_2$ group, are added to an aqueous solution of pyrene, the fluorescence is not quenched. However, when triethanolamine (TEA), bearing a tertiary N atom, was added to an aqueous solution of pyrene, the fluorescence of the latter was quenched as shown in the Stern−Volmer plot of Figure 3 (dotted line). Note that TEA is a well-known quencher of the fluorescence of pyrene.[20] It is clear therefore that the reduction of the fluorescence intensity of pyrene, when it is solubilized in aqueous dendrimer solutions, must be attributed to quenching by the tertiary nitrogens occupying the branching points of all three dendrimers (see Chart 1). From the increased solubilization of pyrene in dendrimer solutions and the quenching of its fluorescence by the tertiary N at the branching points, it is concluded that this fluorophore associates with the dendrimeric structures in water, due presumably to the incorporation of pyrene in the interior of the microcavities of the dendrimers, a fact which has already been observed in other similar systems.[20]

On the basis of the conclusion of complex formation between pyrene and the dendrimer molecules, we have used the dependence of the fluorescence intensity on dendrimer concentration (see Figure 2) in a rigorous nonlinear fitting-curve procedure, to estimate the corresponding association constants. Thus, assuming a 1:1 pyrene/dendrimer complex formed according to eq 1

(20) Herkstroeter, W. G.; Martic, P. A.; Farid, S. *J. Chem. Soc., Perkin Trans. 2* **1984**, 1453.

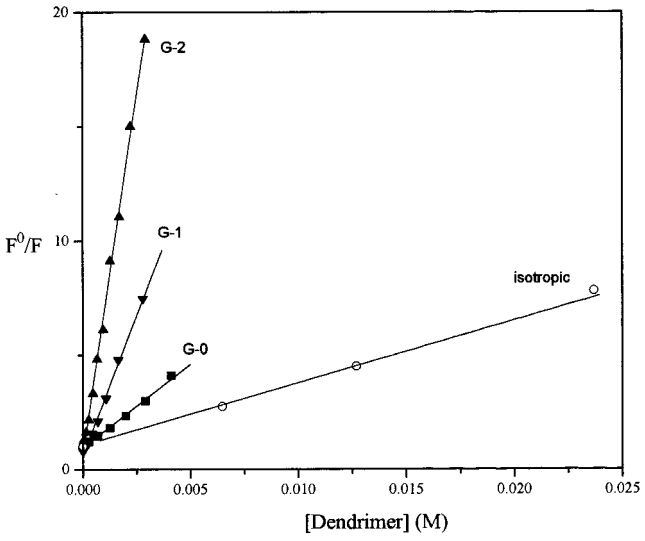


**Figure 3.** Stern−Volmer plots for a pyrene aqueous solution ($8 \times 10^{-7}$M) quenched by dendrimers: ■, G-0; ●, G-1; ▲, G-2. Lines represent the best fitting curves obtained using a linear least-squares fitting procedure.

$$P + D \overset{K}{\rightleftharpoons} PD \tag{1}$$

the binding constant $K$ was obtained by fitting eq 2 to the experimental data of Figure 2

$$K = [PD]/[P][D] \tag{2}$$

where [P] and [D] are the concentrations of the free pyrene and dendrimer, respectively, and [PD] is the concentration of the complex. To obtain the appropriate fitting equation we took into account the mass balance of pyrene (eq 3)

$$[P_0] = [P] + [PD] \tag{3}$$

where $[P_0]$ is the analytical concentration of pyrene, and combining eqs 2 and 3, we arrived at eq 4

$$[PD]/[P_0] = K[D]/(1 + K[D]) \tag{4}$$

We then set

$$f_b = [PD]/[P_0] \tag{5}$$

and

$$f_f = [P]/[P_0] \tag{6}$$

for the molar fraction of the bound, $f_b$, and the free, $f_f$, fluorophore, respectively, where $f_b + f_f = 1$. Obviously the total fluorescence intensity at any moment during the titration is given by eq 7

$$F = f_f F° + f_b F^b \tag{7}$$

where $F°$ is the total initial fluorescence intensity of a pure pyrene aqueous solution and $F^b$ is the total intensity of the pyrene when all of it is bound to the dendrimer. Eventually, by combining eqs 4, 5, 6, and 7 we obtained eq 8

$$F/F° = 1 + \{(F^b/F°) - 1)\}K[D]/(1 + K[D]) \tag{8}$$

which is the fitting function. Note also that since at any instant during the titration the concentration of the added dendrimer is very large compared to that of pyrene, viz., $[D]/[P] \gg 10^4$, [D] in eq 8 can be assumed equal to the

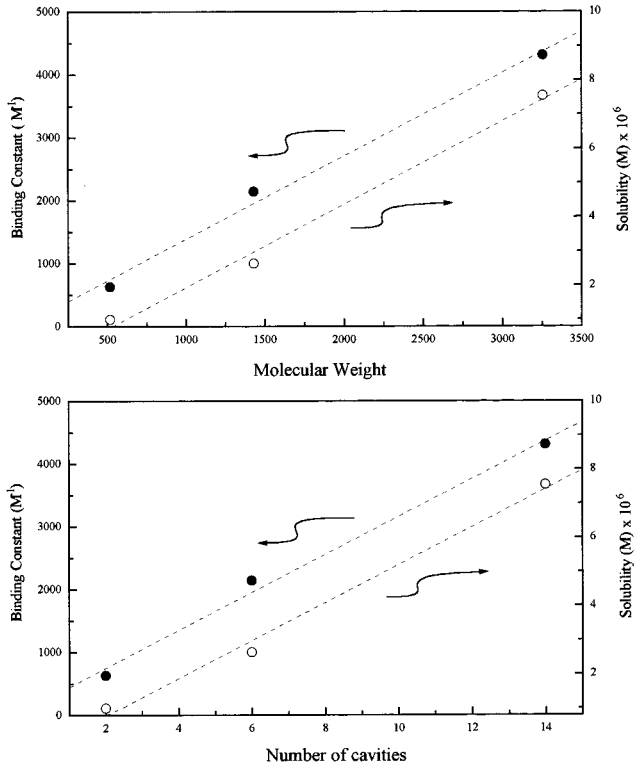


**Figure 4.** Plot of the pyrene−dendrimer binding constants (filled circles) and of the maximum solubility of pyrene in dendrimer solutions (open circles) vs the molecular weight and the number of cavities of the corresponding dendrimer.

analytical dendrimer concentration after every addition of dendrimer throughout the titration. Figure 2 shows the experimental points and the best fitting curves, from which the binding constants estimated for the three dendrimers were $K_{G-0} = 628 \pm 17\ M^{-1}$, $K_{G-1} = 2145 \pm 104\ M^{-1}$, and $K_{G-2} = 4307 \pm 121\ M^{-1}$. The plots of Figure 4 show that the above $K$ values of the binding constants are linearly dependent on the molecular weight and on the number of cavities in each dendrimer. It is also deduced from the same Figure 4 that the maximum solubilities of pyrene in the three dendrimers follow an identical trend, with respect to the dendrimer molecular weight and to the number of cavities, with that of the corresponding binding constants. Furthermore, it is worth mentioning that if $F^b \ll F°$, eq 8, after inversion, assumes the normal form of the Stern−Volmer equation, viz. $F°/F = 1 + K[D]$. Stern−Volmer plots for the quenching of the fluorescence of pyrene in water by the three dendrimers and also by TEA are shown in Figure 3. The slopes of these Stern−Volmer straight lines have the values 670, 2125, 4688, and 273 $M^{-1}$ for quenching with G-0, G-1, G-2, and TEA, respectively. From these slopes and the fluorescence lifetime of pyrene in non-degassed water, which we have found equal to 132 ns, we have estimated the fluorescence quenching rate constants $k_q$ equal to $5 \times 10^9\ M^{-1}\ s^{-1}$ for G-0, $1.6 \times 10^{10}\ M^{-1}\ s^{-1}$ for G-1, $3.5 \times 10^{10}\ M^{-1}\ s^{-1}$ for G-2, and $2.0 \times 10^9\ M^{-1}\ s^{-1}$ for TEA. These large $k_q$ values indicate diffusion-controlled fluorescence quenching in all cases. The increasing $k_q$ with increasing size of the dendrimer reflects the progressively increasing number of quenching sites in G-0, G-1, and G-2. On the other hand, the lowest $k_q$ value found in the case of the isotropic quenching of pyrene by TEA is attributed to the fact that fluorophore and quencher are homogeneously dispersed throughout the solution, instead of being restricted within the limits of the dendrimeric structure as it is the case in the fluorescence quenching in the G-0, G-1, and G-2 aqueous solutions.

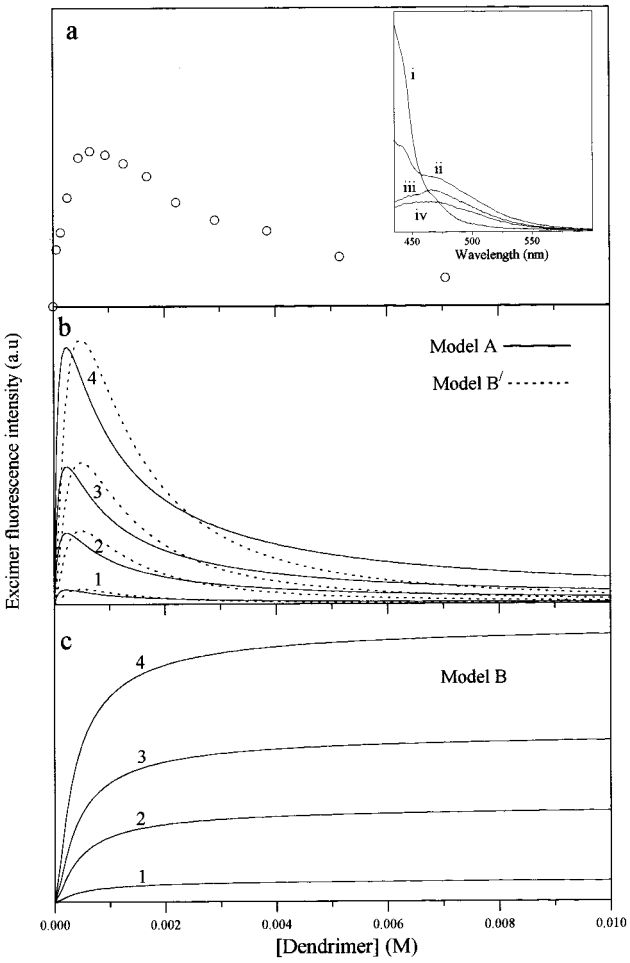


**Figure 5.** (a) Excimer fluorescence intensity of an $8 \times 10^{-7}$ M aqueous pyrene solution vs the concentration of added G-2 dendrimer. Insert: Fluorescence spectra showing the rise and fall of excimer fluorescence at various G-2 concentrations: i, 0.00 M; ii, $4.52 \times 10^{-4}$ M; iii, $5.00 \times 10^{-3}$ M; iv, $7.00 \times 10^{-3}$ M. Simulated curves (b) according to models A and B′ and (c) according to model B. $K = 4307\ M^{-1}$. $K_A$ and $K_B$ take the following values: 1, $10^4\ M^{-1}$; 2, $5 \times 10^4\ M^{-1}$; 3, $1 \times 10^5\ M^{-1}$; 4, $2 \times 10^5\ M^{-1}$.

**Excimer Pyrene Formation.** Under closer examination of the quenching process we found that when G-2 dendrimer is added to the $8 \times 10^{-7}$ M aqueous solution of pyrene, along with the decrease of the monomer fluorescence, some very weak excimer fluorescence appears. The intensity of this weak fluorescence initially increases with addition of dendrimer, until it reaches a maximum value at ca. $6 \times 10^{-4}$ M dendrimer concentration, and then it decreases continuously, as shown in Figure 5a. Assuming Poisson distribution of the pyrene molecules among the dendrimer units, we can estimate that, for the above concentration ratio $[P]/[D] = 8 \times 10^{-7}/6 \times 10^{-4} = 1.33 \times 10^{-3}$, there is a probability equal to approximately $10^{-6}$ that a dendrimer will contain two pyrene molecules, compared to $1.3 \times 10^{-3}$ to contain one pyrene molecule and 0.9987 to be empty. Consequently, the probability for excimers to form in such solutions is practically zero. It is therefore very surprising that excimer fluorescence is at all observed, as it is indeed in Figure 5a. To further investigate this excimer formation we have recorded the excitation spectra of pyrene in an aqueous solution of G-2 dendrimer, at 370 nm (monomer) and 480 nm (excimer). We have observed a red shift of ca. 2.5 nm of the excimer with respect to the monomer excitation spectrum, which suggests the formation of very weakly bound ground state pyrene dimers.[21] Subse-

quently we added to this solution the water soluble quencher TEA and we found that it quenched only part of the monomer pyrene fluorescence—evidently that part of pyrene dissolved in the aqueous phase—while the intensity of the excimer emission was not at all affected. This indicates that the pyrene dimers are formed, as expected, inside the dendrimers where they are protected from water and water soluble species.

There are essentially two rationalizations for this excimer formation. First, for some reason, two pyrene molecules solubilize in the same G-2 dendrimer, where upon excitation they form excimers due to their effective high concentration in the restricted volume of the dendrimer. We call this model A. Second (model B), it is conceivable that two dendrimers, which already host one pyrene molecule each, collide and stick together, thus forming a larger unit which contains two pyrene molecules and therefore excimers can be formed. In order to distinguish between these mechanisms, we have generated simulation curves according to models A and B.

model A

$$P + D \overset{K}{\rightleftharpoons} PD$$

$$P + PD \overset{K_A}{\rightleftharpoons} P_2D$$

model B

$$P + D \overset{K}{\rightleftharpoons} PD$$

$$PD + PD \overset{K_B}{\rightleftharpoons} P_2D_2$$

Note that we have produced only simulated curves of models A and B and not rigorous fittings to the data, because the changes of the excimer intensity are really small (see insert in Figure 5a), therefore accurate estimation of their values, proper for a least-squares fitting, is impossible. According to model A the excimer fluorescence intensity is analogous to the concentration $P_2D$, whereas according to B it is analogous to $P_2D_2$. Analytical expressions for these two concentrations, $[P_2D]$ and $[P_2D_2]$, can be extracted from eqs 8 and 9, having first obtained expressions for [P] from eqs 10 or 11, which describe the mass balance of pyrene in model A and B, respectively.

$$[P_2D] = K_A K [P]^2 [D] \quad (8)$$

$$[P_2D_2] = K_B K^2 [P]^2 [D]^2 \quad (9)$$

$$2KK_A[D][P]^2 + (1 + K[D])[P] - [P]_0 = 0 \quad (10)$$

$$2K^2K_B[D]^2[P]^2 + (1 + K[D])[P] - [P]_0 = 0 \quad (11)$$

For these simulations we have varied the concentration of the dendrimer, at constant pyrene concentration $[P]_0 = 8 \times 10^{-7}$ M, we have used the binding parameter for the $P + D \rightleftharpoons PD$ complexation, $K_{G-2} = 4307\ M^{-1}$, obtained from the fittings of Figure 2, and we have assigned varying values to $K_A$ and $K_B$. On comparison of parts b and c of Figure 5, it becomes evident that the simulated curves generated from model A (Figure 5b) closely resemble the behavior of the experimental data shown in Figure 5a. We therefore conclude that $P_2D$ must be the predominant species which is responsible for the excimer appearance in the pyrene–dendrimer system. A similar situation, but less pronounced, we have also observed in the cases of G-0 and G-1 dendrimers.

However, model B can be modified in a way that it also gives rise to simulations in agreement with the experimental data. Thus, if in addition to the two interactions of model B, we assume a third one, viz., the association of PD with one dendrimer molecule, we obtain model B′, which produces the simulations of Figure 5b (dotted lines) in good agreement with experiments.

model B′

$$P + D \overset{K}{\rightleftharpoons} PD$$

$$PD + PD \overset{K_B}{\rightleftharpoons} P_2D_2$$

$$PD + D \overset{K_{B'}}{\rightleftharpoons} PD_2$$

There is though one more requirement that model B′ should fulfill. This is the fact that a plot of $F°/F$ vs [D] must produce a straight line, similar to the straight lines of Figure 3. In other words at this low pyrene concentration the amount of excimer formed is very small (see insert Figure 5). It is therefore a good approximation to ignore the excimer fluorescence and simplify model B to model B′.

reduced model B′

$$P + D \overset{K}{\rightleftharpoons} PD$$

$$PD + D \overset{K_{B'}}{\rightleftharpoons} PD_2$$

It is easily shown that according to the reduced model B′ the relationship between $F°/F$ and [D] is given by eq 12,

$$F°/F = 1 + K[D] + KK_{B'}[D]^2 \quad (12)$$

which evidently cannot be made to fit to the straight lines of the experimental data shown in Figure 3. Even for a very low value of $K_{B'}$, e.g., 10 $M^{-1}$, the plot of $F°/F$ vs [D] according to eq 12 deviates from a straight line much more than the experimental error.

Finally model B, viz., that the excimer emission is due to the formation of dimeric (or larger) dendrimer aggregates containing two or more pyrene molecules, was excluded by light scattering measurements. Thus two $5.0 \times 10^{-3}$ M aqueous solutions of G-2 dendrimer, the one saturated with pyrene and the other without any pyrene in it, gave a mean molecular weight for the particles in both solutions equal to 3215, which is in very good agreement with 3256, the molecular weight of the monomeric G-2 dendrimer. Our conclusion therefore is that only model A explains the experimental data of Figure 3 and Figure 5a.

So far, we have discussed the fluorescence of solutions having low and constant pyrene concentration, viz., $8 \times 10^{-7}$ M, and varying amounts of dendrimers. We will now examine the reverse situation where the dendrimer concentration is kept constant while that of pyrene increases. Such is the case of Figure 6, which shows the total emission of pyrene (from $1.59 \times 10^{-6}$ to $7.55 \times 10^{-6}$ M), solubilized in $10^{-2}$ M aqueous solution of G-2. It is evident from this figure that the excimer fluorescence increases as the concentration of pyrene increases and this is the behavior expected from model A. Note that in this [P]/[D] range Poisson distribution also predicts

(21) Winnik, F. M. *Chem. Rev.* **1993**, *93*, 587.

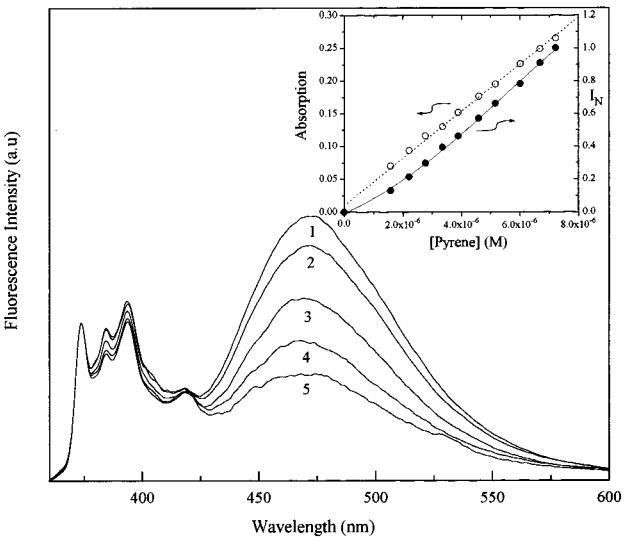


**Figure 6.** Total fluorescence from $10^{-2}$ M aqueous solution of G-2, containing various concentrations of pyrene: 1, $7.23 \times 10^{-6}$ M; 2, $6.02 \times 10^{-6}$ M; 3, $3.9 \times 10^{-6}$ M; 4, $2.29 \times 10^{-6}$ M; 5, $1.59 \times 10^{-6}$ M. The spectra have been normalized at the first pyrene emission peak (374 nm). Insert: Plot of the optical density of pyrene (open circles), and of the corresponding fluorescence ratio $I_N = I_{ex}/I_{ex}^{max}$ (see text) (filled circles) as a function of added pyrene.

vanishingly small double occupation of dendrimers by pyrene molecules, nevertheless the excimer fluorescence predominates, as clearly seen in Figure 6. We have excluded the possibility that as the concentration of pyrene increases microcrystals or other pyrene aggregates form in the solution by confirming the validity of Beer's law, i.e., the linear dependence of optical density on the concentration of pyrene, as shown in the insert of Figure 6. On the basis of the mechanism of Chart 1 it is possible to fit eq 13 to the experimental data of the excimer intensity $I_{ex}$ at various pyrene concentrations and constant [D] = $10^{-2}$ M. Note that the fitting of eq 13 was derived in a straightforward manner from eqs 8−11.

$$I_N = \frac{I_{ex}}{I_{ex}^{max}} = \left(\frac{[P]_{free}}{[P]_{free}^{max}}\right)^2 \qquad (13)$$

In this equation $[P]_{free}^{max}$ stands for the free pyrene concentration—i.e., the concentration of pyrene which is not associated with dendrimers—in a [D] = $10^{-2}$ M aqueous solution of dendrimer G-2 saturated with pyrene ($[P]_{tot}^{max} = 7.55 \times 10^{-6}$ M for G-2), and $[P]_{free}$ is the free pyrene concentration at any moment through the dilution process (dilution of the pyrene aqueous solution by a $10^{-2}$ M aqueous solution of dendrimer). $I_{ex}^{max}$ is the maximum value of the excimer fluorescence obtained during the dilution process. $I_{ex}$ and $I_{ex}^{max}$ are measured directly from the fluorescence spectra, whereas $[P]_{free}$ and $[P]_{free}^{max}$ are calculated from eqs 14 and 15, which combine the expression for the mass balance of pyrene with the expressions for the binding constants $K$ and $K_A$.

$$[P]_{tot} = 2KK_A[P]_{free}^2 + (1 + K_A D_0)[P]_{free} \qquad (14)$$

$$[P]_{tot}^{max} = 2KK_A([P]_{free}^{max})^2 + (1 + K_A D_0)[P]_{free}^{max} \qquad (15)$$

By setting [D] = $10^{-2}$ M and $K = 4307$ $M^{-1}$ (obtained from the previous fit of eq 8 for G-2, see Figure 2), the fitting gave $K_A = 1.6 \times 10^5 \pm 1.4 \times 10^4$ $M^{-1}$ with a correlation coefficient 0.9998.

At this point we should emphasize the possibility that what we have called excimer could instead be some kind of exciplex formed between pyrene and some chemical entity inside the dendrimer, e.g., the tertiary amine N atoms at the branching points of the dendrimer structure. To investigate this possibility, we have examined the fluorescence spectra of pyrene in TEA to simulate the effect of the tertiary amine group at the branching points, in ethylenediamine to simulate the effect of the $NH_2$ terminal groups, and in biacetylethylenediamine to simulate the effect of the basic repeat unit (see Chart 1). The only effect we observed in these cases was the quenching of the fluorescence of pyrene in TEA. Moreover, when HCl was added to an aqueous solution containing $7.55 \times 10^{-2}$ M pyrene and $10^{-2}$ G-2 dendrimer, the fluorescence, monomer and excimer, increased as much as 5−6 times. This increase of the fluorescence intensity we have attributed to the protonation, by the $H^+$ cations, of the lone electron pair on N at the branching sites, which causes the quenching. In the case of excimer formation one would expect increase of the intensity of the excimer fluorescence, along with the monomeric, when the quenching group is neutralized by protonation. On the contrary, exciplex formation between pyrene and the tertiary amine group should be diminished upon protonation, in view of the important role of the lone electron pair in such processes. Our results show that both monomer and excimer fluorescence of dendrimer-solubilized pyrene increase upon addition of HCl. We tend to accept therefore that exciplex formation, at least between pyrene and the chemical groups at the branching points, is rather unlikely. In view of the additional fact that the excimer emission from the dendrimer solution overlaps exactly ordinary excimers formed in concentrated solutions, the alternative of excimer formation seems more favorable than that of exciplex. However, our findings do not eliminate all the possibilities for exciplex formation inside the microcavities of these dendrimers. Further studies of this problem are now under way, involving other dendrimers structures as well as $\gamma$-cyclodextrin.

## IV. Conclusions

The main conclusions drawn from the present study of these new materials can be summarized as follows: (a) As the dendrimer grows in size the amount of pyrene solubilized is increased linearly with respect to the dendrimer molecular weight, and to the number of cavities. (b) The larger the dendrimer the better is pyrene protected from the bulk water phase. (c) When pyrene is associated with dendrimers in aqueous media, its fluorescence is quenched by the tertiary N present at the branching points of the dendrimers. (d) When pyrene is solubilized in aqueous dendrimer solutions, excimer fluorescence is observed even at concentrations at which, according to Poisson distribution, there is a negligible probability for double pyrene occupation of a dendrimer unit. It is however plausible that exciplexes are formed between pyrene and some part of the interior of the dendrimer. The binding constant for this excimer (or exciplex) formation is equal to $1.6 \times 10^5 \pm 1.4 \times 10^4$ $M^{-1}$ in the case of the G-2 dendrimer.

**Acknowledgment.** The authors wish to acknowledge the assistance of Dr. J. Poulos of the University of Athens, with the light scattering experiments.

LA970529I